Available online at website: https://journal.bcrec.id/index.php/bcrec

Bulletin of Chemical Reaction Engineering & Catalysis, 19 (3) 2024, 500-511

Research Article

Kinetic Insights into Solar-Assisted Fabrication and Photocatalytic Performance of $CoWO_4$/NCW Heterostructure

Ali A. Hassan[1,2,3*], Ibtehal Kareem Shakir[3]

[1]*Department of Chemical Engineering, College of Engineering, University of Muthanna, Muthanna, Iraq*
[2]*Department of Petroleum Engineering, College of Engineering, Al-Ain University, Thi-Qar, Iraq*
[3]*Department of Chemical Engineering, College of Engineering, University of Baghdad, Baghdad, Iraq*

Received: 17th August 2024; Revised: 21th September 2024; Accepted: 22th September2024
Available online: 12th October 2024; Published regularly: October 2024

Abstract

This work studies the kinetic model for the solar-driven fabrication of $CoWO_4$/NCW heterostructure photocatalysts and investigates their enhanced photocatalytic degradation activity. The synthesis of $CoWO_4$/NCW, its characterization, and the kinetic aspects of photocatalytic degradation under solar light. New nanocomposite prepared from Nano cellulose (NCW) by hydrolysis cotton waste (CW) by nitric acid and cobalt tungstate ($CoWO_4$) prepared from sodium tungstate and cobalt chloride by wet chemical method and characterized through XRD, FTIR, EDX, and FE-SEM analyses. The composite's performance in organic oxidation from refinery wastewater (RWW) was evaluated under solar light. The high removal ratio was 97.4% for organic pollutants (OP) in refinery wastewater. The results indicate that the heterostructure exhibits improved photocatalytic performance compared to individual components, which kinetics model was the best to represent the photocatalytic degradation of organic pollutants from oily wastewater over the heterostructure $CoWO_4$/NCW catalyst. Add future applications of this finding in the relevant industries.

Keywords: water treatment; solar energy; photocatalytic; characterization; batch oxidation reactor

How to Cite: A.A. Hassan, I.K. Shakir (2024). Kinetic Insights into Solar-Assisted Fabrication and Photocatalytic Performance of $CoWO_4$/NCW Heterostructure. *Bulletin of Chemical Reaction Engineering & Catalysis*, 19 (3), 500-511 (doi: 10.9767/bcrec.20198)

Permalink/DOI: https://doi.org/10.9767/bcrec.20198

1. Introduction

Over the last decade, as industrialization has accelerated, people have become progressively concerned about the pollution of water [1]. In our country, several treatment wastewater methods, for instance photo-oxidation degradation [2], electro-catalytic degradation [3], adsorption [4-5], and biodegradation [6], are used to solve the difficulties. Photocatalytic materials are particularly popular since they can directly apply solar energy and have the assistance of no secondary contamination and easy reprocessing [7]. In recent years, it has developed the primary paper topic. Aside from removing contaminants, photo-oxidation can be used to resolve the energy shortage problem [8]. An ecologically sociable approach must be designed to perform squalor reactions more exactly and professionally to eliminate these poisonous chemicals from wastewater [9].

Previously used conservative approaches were not proven to be appropriate due to their difficulty, low competence, time-consuming mechanisms, disposal subjects, and inefficient nature [10-11]. Solar energy is widely observed as a well-organized, readily obtainable, and suitable energy source on the abundantly available. Visible light provides 43% of the solar spectrum's energy, while the UV region contributes only 4% [12]. In this respect, the growth of active photo-catalysts, particularly visible light-responsive schemes, is

* Corresponding Author.
Email: ali.alkhafaji@mu.edu.iq (Ali A. Hassan)

critical for the efficient use of sunlight-based energy in photocatalysis [13].

These charged species play a significant role in photocatalysis by providing a surface for species adsorption and generating superoxide and free radicals, which further participate in oxidation-reduction degradation reactions [14]. Tungsten trioxide (WO_3), chosen as the semiconductor for etching into a photocatalyst, is an n-type semiconductor due to its advantageous physical and chemical properties [15]. Its distinguishing feature is a relatively small bandgap (ranging from 2.4 to 2.8 eV), as opposed to photocatalysts such as TiO_2 and ZnO were larger bandgap (3.2 to 3.37 eV) [16]. To gain a deeper comprehension of $CoWO_4$'s photocatalytic activity, we have examined the impact of diverse light irradiations, including solar, visible, and ultraviolet light. TiO_2 that is sold commercially was used to compare the photocatalytic activity. As far as we are aware, this is the first proof that $CoWO_4$ can effectively act by way of a photocatalyst in the degradation of organic contaminants when exposed to UV, visible, and solar light [17].

As a result, improving WO_3's photocatalytic activity requires addressing the aforementioned defects. In recent decades, many reviewers have been devoted to the examination and growth of some effective organizations to solve such glitches, counting morphology engineering, metal-nonmetal doping, defect construction, and heterojunction construction [18]. In this work, $CoWO_4$/NCW nanocomposites were created using a wet chemical method. The materials' structure and properties were described and analyzed. The solar catalytic degradation model performance of nanocomposites against organic pollutants was investigated to determine their activity, stability, and applicability.

2. Materials and Methods

2.1 Wastewater and Analytical Test

Refinery wastewater was conserved at (6 °C) to be treated through the treatment technologies obtained from oilfields refinery and listed in Table 1. All chemicals used in this work were of analytical grade and pure state. Cotton waste was composed from couture workshops and exposed to cutting and shredding procedures and washing with cold and hot water for purification. Sulfuric and Nitric acids (99% purity), NaCl, CCL_4, H_2O_2 (45 %wt. German), NaOH (Thomas barker), Sodium tungstate (99%), and Cobalt chloride hexa hydrate (98% purity) used for wet chemical methods. The absorbance was measured with a UV-1800 spectrophotometer, and the organic concentration in ppm was calculated using the standard curve [19]. The organic elimination efficacy was assessed:

$$Y_{OC} = \frac{C_o - C_t}{C_o} \times 100\% \quad (1)$$

where, C_o and C_t are the initial and final concentration in RWW, respectively.

Table 1. Properties of refinery wastewater

Limits	Values	Limits	Values
Organic concentration	165.3 (mg/L)	Conductivity	432531 µs/cm
Turbidity	21.12 NTU	TDS	276819.84 (mg/L)
pH	6.85	Viscosity	1.02 m Pa/S

2.2 The Preparation of Nano Cellulose

The cotton waste was washed with cold and hot water for purification from wastes impregnated in a 5 % NaOH solution and stirred incessantly [20]. The CW was dried at 70 °C in an oven for 1 day to comprehensive the procedure of washing. Subsequently, the CW was in a solution containing 2/7 % acetic acid and hydrogen peroxide [21]. The prepared Nano cellulose from added cotton waste to mixed 15/20 mL solution of concentrated HNO_3 and distilled water, heated at 40 °C with constant stirring for 3 hours to ensure thorough mixing. The subsequent mixture was washed numerous times with water until a neutral pH was reached as exposed in Figure 1.

2.3 Synthesis of $CoWO_4$/ NCW Nanocomposite

The composite prepared by the wet-chemical method, $CoWO_4$ nanoparticles are supported on NCW, with some adjustments to the preparation temperature, following methods reported in the literature [22]. One-half grams of NCW was ultra-sonicated in 100 mL of distilled water for 25 minutes, the suspension was stirred for an additional 30 minutes to ensure thorough mixing 0.225 grams of cobalt chloride were added to the NCW suspension. Twenty-five milliliters of the sodium tungstate solution was slowly added to the Nano cellulose suspension containing cobalt chloride under stirring.

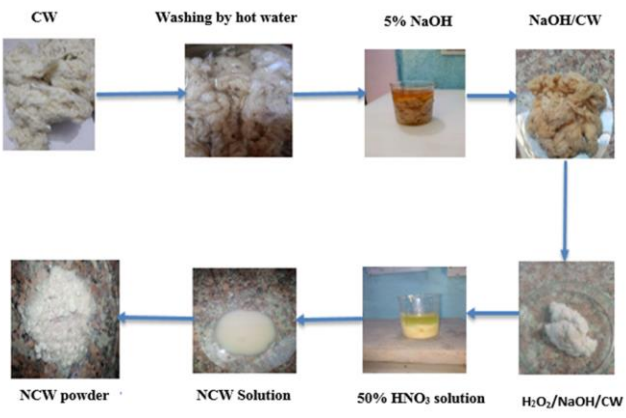

Figure 1. The preparation of NCW

This step ensures thorough mixing and promotes the formation of the nanocomposite. The reaction mixture, now containing NCW-supported cobalt tungstate composite, was refluxed at 95 °C for 3 h. The nanocomposite was washed numerous times with alcohol and distilled water to eliminate any residual reactants or by-products. Lastly, the purified nanocomposite was dried overnight at 60 °C to remove any remaining solvent and obtain the final product used in work solar degradation.

2.4 Characterizations

New composites were characterized using analytical methods to determine their structural, morphological, structural, and thermal properties. FTIR analysis (FTIR-2000, Bruker) was performed in the 4000 to 400 cm^{-1} range using the Attenuated Total Reflectance method .FE-SEM (SUPRA55VP) was used to examine the surface morphology of the composite adsorbent. XRD analysis (Model MDK 2 TESLA) confirmed the NCW preparation and their presence in $CoWO_4$/NCW composites.

2.5 Batch Adsorbent / Solar Degradation

The solar degradation experiments were carried out in a batch oxidation reactor, which is a vessel designed with 250 ml containing 150 mL of refinery wastewater for conducting experiments in a controlled atmosphere. A magnetic stirrer was used to ensure that the RWW was evenly mixed within the nanocomposite in the reactor. Before adding the composite, the RWW's pH was adjusted with dilute basic or acid solutions. pH adjustment is critical because it affects the adsorption capacity and effectiveness of the treatment process. Figure 2 depicts the refinery wastewater treatment setup using sunlight as the visible light source. It could include the adsorbent composite used for OP removal as well as the solar light, which is where the solar degradation process occurs.

3. Results and Discussion

3.1 The Characteristics of $CoWO_4$/NCW

The oxidation reaction has a notable impact on the structure of CW, NCW, and $CoWO_4$/NCW, as evidenced by FT-IR spectroscopy. In the FT-IR spectroscopy analysis presented in Figure 3, the range from 3000 cm^{-1} to 3600 cm^{-1} resembles–OH stretching feelings, which are primarily owing to the abundance of hydroxyl groups in cotton waste and other composites [23]. The little change in the absorption band ranges from 900–1500 cm^{-1} because of NCW absorption indicated at some shifted bands. The band of 710 cm^{-1} refers to C–O in-plane winding and C–H aromatics, 1012.11 cm^{-1} states to C–H bending and C–O stretching, and 1447.33 cm^{-1} is assigned to C=C stretching and is associated with native cellulose. The bands that appeared in the area 2465.44–1723.55 cm^{-1} are responsible for the symmetric extending vibrations strength Following oxidation, the relative intensities in this range reduction, are representative of an important reduction in the content of hydroxyl groups [24]. Regarding XRD analysis in Figure 4, the characteristic peaks of the NCW sample are consistent with standard peaks of nano cellulose [25]. The absence of substantial changes to the XRD planes suggests that the particles are effectively synthesized and well-formed, demonstrating high crystallinity,

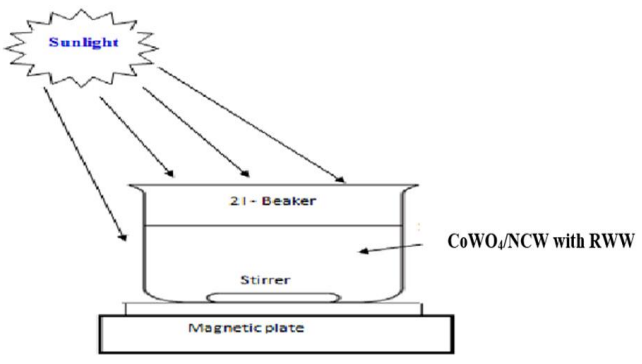

Figure 2. The solar degradation for RWW

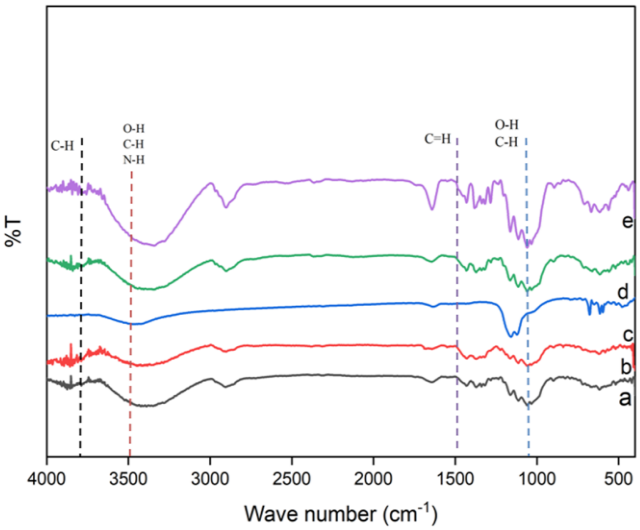

Figure 3. FTIR analysis of (a) CW, (b) NaOH/CW, (c) H_2O_2/NaOH/CW, (d) NCW, and (e) $CoWO_4$/NCW

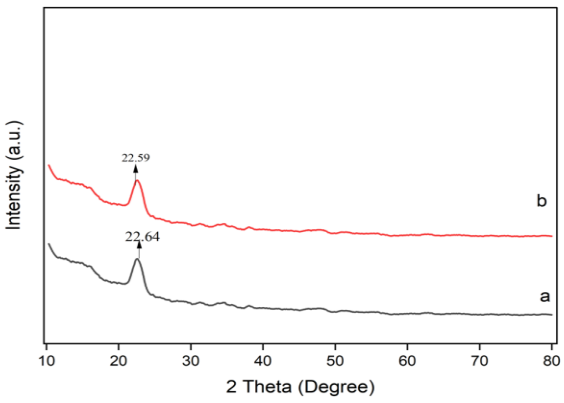

Figure 4. XRD patterns of NCW and new composite

Sharp peaks are observed at 2θ = 22.59, indicating the typical pattern of type I cellulose for NCW. For $CoWO_4$, an amorphous structure is observed, with characteristic diffraction peaks similar to those of a $CoWO_4$ sample prepared by Shekofteh *et al.* [26]. The particles exhibit a nanocrystal line structure with a polyhedral shape, nearly hexagonal or spherical-like, and homogeneous [27]. The morphological structures and surface characteristics of cotton waste and composite materials are frequently studied using FE-SEM. As seen in Figure 5, it also displays the porosity and surface texture of the new composite from cobalt tungstate and nano cellulose. $CoWO_4$ appears by way of a rod because of the refluxing procedure, contrasting with its amorphous entrance in some studies [28]. EDX analysis was conducted to assess the purity of NCW and $CoWO_4$/NCW presented in Figure 6 for NCW and nanocomposite. The analysis revealed the presence of Co, W, C, and O elements in the samples [22], as listed in Table 2.

3.2 Optimization and Main Effect of Organic Removal

The effect of cobalt tungstate on the Nano cellulose and nanocomposite prepared for organic

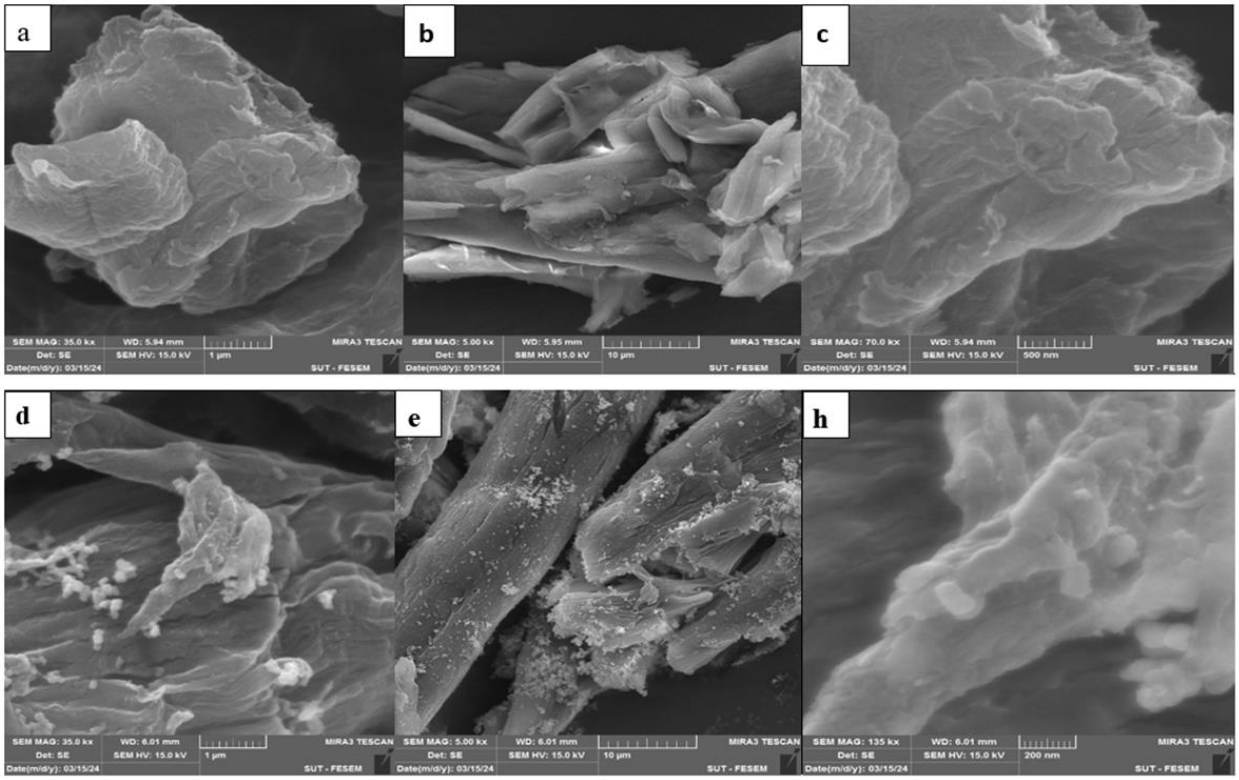

Figure 5. (a) NCW at 1 µm, (b) NCW at 10 µm, (c) NCW at 200 nm, (d) $CoWO_4$/NCW at 1 µm, (e) $CoWO_4$/NCW at 10 µm, (f) $CoWO_4$/NCW at 200 nm

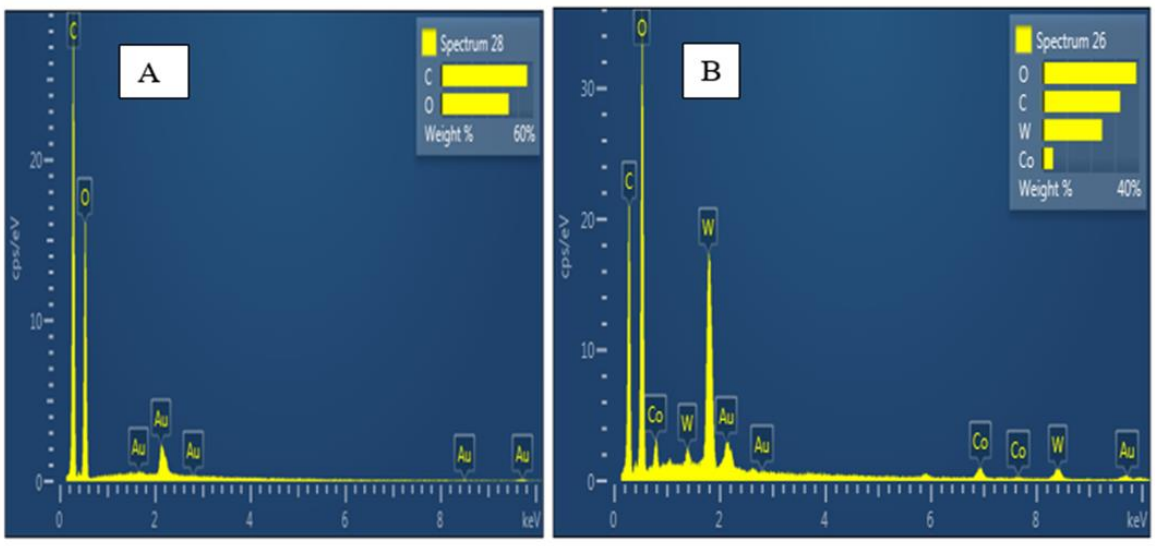

Figure 6. (a) EDX for waste cotton, (b) EDX for $CoWO_4$/NCW

elimination in RWW with different variables of time, pH, dose, and temperature is presented in Figure 7. Extended solar times improved the solar degradation of organic pollutants in RWW. The relationship between organic elimination and reaction time along adsorption/solar degradation is presented in Figure 7a. The results were reliable with previous research, by way of established through prepared nanocomposite with a lower band gap. At levels of high pH, the prepared nanocomposite surface may become protonated, following in a positive charge of the surface leading to augmented adsorption onto the surface of the Nano cellulose and compared with nanocomposite [18]. The influence of pH on Nano cellulose adsorption organic with cobalt tungstate to enhance the oxidation was investigated throughout a pH range of 3 to 9 with a time of 120 minutes with all experiments performed. Figure 7b demonstrates that the greatest efficiencies for $CoWO_4$/NCW, and NCW were 88.4, and 77.2%, respectively at pH of 9.

As a result, a higher dose increases the removal of organic pollutants from the RWW, and cumulative the dose of the composite can result in more efficient utilization of the irradiation source of solar. Figure 7c indicates that organic sorption increases rapidly as the dose increases due to the obtainability of more functional groups and thus more exchangeable surface sites accessible to form complexes with organic contaminants [26]. Figure 7d the data illustrates the removal competence of organic pollutants in RWW for experiments conducted at different temperatures, demonstrating the positive influence of temperature. Specifically, the increase in temperature from 25 °C to 70 °C resulted in enhanced removal efficiency, the removal efficiency rises from 70.5, 81.1 to 76.2, and 87.2 % at low and high temperatures for nano cellulose and composites, respectively [28].

The ideal experimental conditions for the $CoWO_4$/NCW system to achieve the best results for working parameters such as composite dose, pH, solar time, and temperature. Figure 8 illustrates the measurement implications of D-optimization. The maximum organic removal efficiency was 97.4 % at 120 min, pH of 9, dose of 1.5, and 70 °C for $CoWO_4$/NCW. Figure 9 shows the main effects plots of the best combination of

Table 2. EDX for CW and $CoWO_4$/NCW

Element	CW		$CoWO_4$/NCW	
	wt%	Atomic %	wt%	Atomic %
C	55.97	62.87	32.11	50.37
O	44.03	41.81	38.80	45.69
Co			4.42	1.41
W			24.66	2.53
Total	100.00	100.00	100.00	100.00

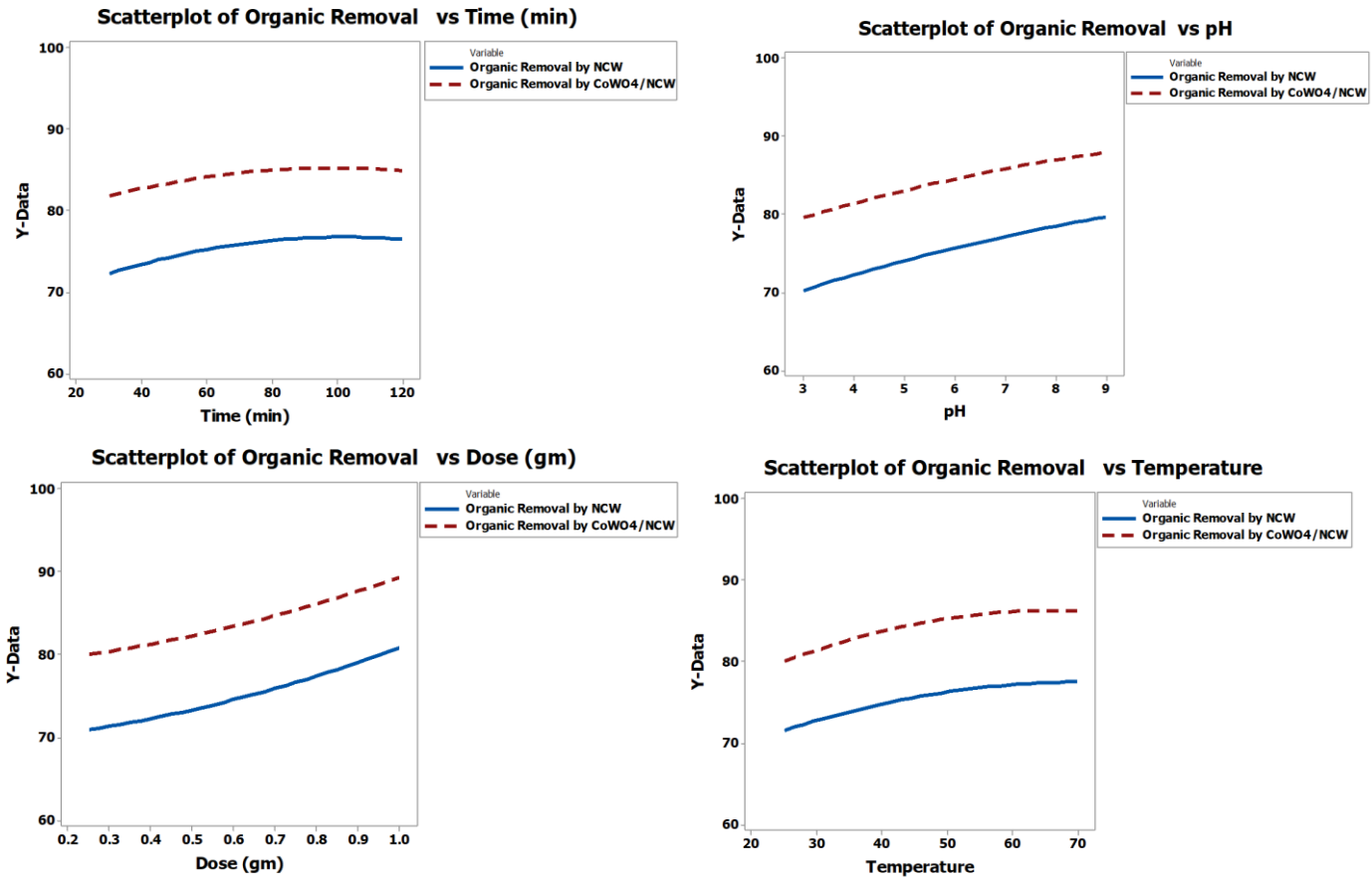

Figure 7. The effect of independent on organic removal (a) time, (b) pH, (c) dose and temperature of (d)

critical limits aimed at attaining the desired adsorption/oxidation performance for the new composite. Each plot demonstrates the best combination of working for an exact presentation of combined treatment. Previous studies have consistently shown that OP increases with increased levels of all independent variables in the research [29].

3.3 Mathematical Model of Batch Reactor for Organic Oxidation

The mathematical model usually describes the dynamic behavior of the system through a set of equations, such as ordinary differential equations, that relate process parameters. Mathematical models are used not only to explain the system but also to study the effects of various components on the system and to find solutions for most problems [30]. By combining oxidation and adsorption were degrade a wider range of organic pollutants in RWW more efficiently. Oxidation can degrade micro molecules into simpler forms, which are then more effortlessly adsorbed onto NCW surfaces. Nanocellulose involves the attachment of organic pollutants from RWW onto a solid surface (nanocellulose). Utilizing both methods together can provide a more complete elimination of OP from RWW or air by leveraging the strengths of each process [31].

The organic removal in refinery wastewater is a multifaceted procedure connecting numerous separate problems to distinguish reactions. So, estimated kinetics aimed at the organic removal of wastewater solution can be presumed. The oxidation mechanism of organic pollutants over the new composite solar catalyst consists of several steps, each of which is enabled by a specific constituent of the heterostructure. When exposed to solar light with energy identical to or better than its band gap energy in the reactor, the solar catalyst is photo-excited, resulting in electron-hole pairs (e_{CB-} and h_{VB+}). The process is described by Equation (2).

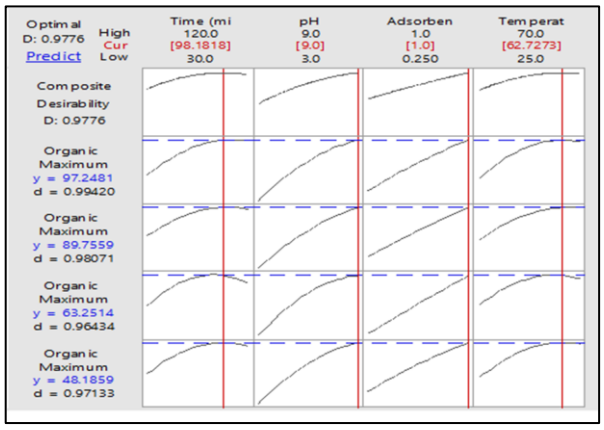

Figure 8. Finest employed variables on refinery wastewater

$$CoWO_4/NCW + (\text{solar light}) \rightarrow CoWO_4/NCW\ (e^- + h^+) \quad (2)$$

The relation between $CoWO_4$ and NCW is critical to solar degradation. They generate an electric field and a difference in band energy potentials, permitting solar-generated electrons to migrate from $CoWO_4$ to nano cellulose and holes from NCW to $CoWO_4$. Photo-generated electrons react with oxygen molecules (O_2^-) to yield oxygen radicals ($O_2^{\bullet -}$), by way illustrated in Equation (4), whereas holes react with adsorbed water and hydroxide ions (OH^-) to produce hydroxyl radicals ($^{\bullet}OH$), as illustrated in Equations (3)–(5).

$$H_2O + h_{VB}^+ \rightarrow \bullet OH + H^+ \quad (3)$$
$$O_2 + e_{CB}^- \rightarrow O_2^{\bullet -} \quad (4)$$
$$O_2^{\bullet -} + H_2O \rightarrow \bullet OH + OH^- + O_2 + HO_2^- \quad (5)$$

Because of their high reactivity and brief half-life, free radicals are produced when organic materials undergo heterogeneous oxidation processes. The following reaction illustrates how hydroxyl radicals react with organic pollutants [32].

$$OH^{\bullet} + R\text{–}H \rightarrow H_2O + R^{\bullet} \quad (6)$$

The dose, pH of the solution, the starting contaminant concentration, and the presence of additional ions are the primary factors influencing the oxidation process [33]. Meanwhile, radicals recombine, as exposed in Equation (7):

$$2^{\bullet}OH \rightarrow H_2O_2 \quad (7)$$

In most real-world situations, such a complicated procedure is not necessary. Because oxidation products are readily degraded, their toxicity is not an issue [34]. To simplify the description of the system, the following assumptions were taken into account for oxidation processes in the batch reactor. The reactor is perfectly mixed to obtain a uniform distribution of the concentration and temperature throughout the reactor, the reaction is isothermal and occurs at atmospheric pressure, the density and heat capacity of all components are constant, and the

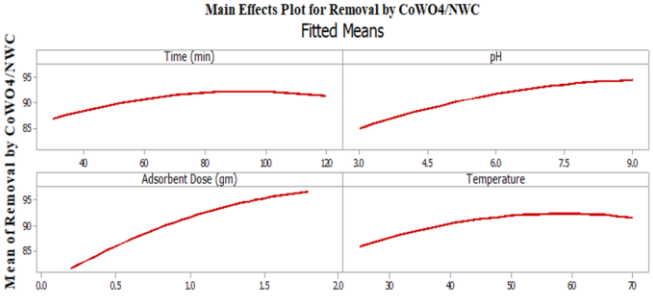

Figure 9. Main effects plot for oil elimination

particle is a sphere Assume the porosity = 0.5. The conservation of mass, continuity, and energy laws was the basis for developing the mathematical model of a batch reactor [35].

[Rate of accumulation within the system] = [Rate of flow into the system] − [Rate of flow out the system] − [Rate of Consumption by chemical reaction within the system] (8)

Total continuity equation for the reaction mass in the batch operation:

The inflow and outflow = 0

Rate of accumulation = $\frac{d(\rho V)}{dt}$

Substituting all these terms in Equation (8), the continuity equation of the batch reactor will be:

$\frac{d(\rho V)}{dt} = 0 - 0$ (9)

Since ρ of the mixture is constant, according to Equation (8) $dV/dt = 0$, so the liquid volume in the batch reactor is unchanged (constant).

Mole balance for organic component (O):

The inflow and outflow = 0

Rate of disappearance of component (O) = $(-r_O)V$

Rate of accumulation of component (O) $= dN/dt$

$dN/dt = -(-r_O)\ V$

$dN/Vdt = r_O$

$dC/dt = r_O$ (10)

When a hydrogen atom is removed from an organic pollutant, Equation (6) predicts the formation of water, R˙ (alkyl radical) , volume of solution (V) in mL, number of moles (N) in gmol, the rate of oxidation (r_O) and organic concentration (C) in ppm. The measurement of the above equation's reaction constant rate is difficult because the concentration of the free radical cannot be stated. A pseudo-first or second-order approximation is an alternative solution to this problem. Because only one of the reactants in the reaction is specified, the reaction rate coefficient (K) is referred to as the apparent constant rate (k_{app}) in min^{-1} (Equation 11).

$$r_O = k[\bullet OH][RH] = k_{app}[RH] = k_{app}C = -\frac{dC}{dt} \quad (11)$$

Using linear regression analysis, the kinetic models for the breakdown of organic pollutants at different processes were computed. This study used pseudo-first and second-order reaction kinetics to examine the kinetics of organic degradation with hydroxyl radical. Subsequently, the outcomes were juxtaposed and the kinetic model exhibiting the best fit was identified. The OH˙ that attacks and initiates the oxidation of molecule organic contaminants (R) through numerous mechanisms of degradation by way of seen below (Eqs. (12)–(15)) [36].

The first-order (K_1) model in min^{-1} and second-order model (K_2) in (mL/mol.min), respectively [37]:

$$-\frac{dC}{dt} = K_1 C \quad (12)$$

$$ln\frac{[C_0]}{[C_t]} = K_1 t \quad (13)$$

$$-\frac{dC}{dt} = K_1 C^2 \quad (14)$$

$$\frac{1}{[C_t]} - \frac{1}{[C_0]} = K_2 t \quad (15)$$

A plot of $\ln(C_o/C)$ and $(1/C\text{-}1/C_o)$ versus time (t) for each test leads toward a straight line whose slope is K_1 and K_2, respectively. Because of its simplicity and strong agreement for a specific initial organic content, the first-order kinetic has been widely used in both heterogeneous and homogeneous oxidation processes (Equation (13)). As a result, it is critical to comprehend the impact of effective operational parameters, such as the initial concentration of pollutants, on the removal rate. The constant of the reaction rate is influenced by the reaction temperature and can be determined by the Arrhenius equation, which is expressed by Equation (16) [35].

$$k_1 = k_0 e^{-E/RT} \quad (16)$$

Substitute Equation (16) in Equation (11), we get:

$$-\frac{dC}{dt} = K_0 e^{-E/RT} C \quad (17)$$

where, K_1 and K_o the first order constants in min^{-1} for variable and 25 °C, respectively. The activation energy (E) in J/mol, temperature (T) in Kelvin, and R is the gas constant in J/mol.K.

Holes can directly oxidize organic pollutants in RWW. The produced species of reactive oxygen, which comprise oxygen radicals and free radicals, in addition to direct oxidation by holes, aid in the degradation of OP in the oxidation system. Figure 10 visually depicts these steps, counting the migration of electrons and holes, the production of reactive oxygen species, and the subsequent degradation of organic pollutants over the solar catalyst under visible light irradiation [38].

The kinetics of the organic sorption process $CoWO_4$/NCW were investigated using pseudo-first-order and pseudo-second-order kinetic models. The pseudo-first-order kinetics equation was found to provide a better fit compared to the pseudo-second-order equation. Linear plots were obtained with the pseudo-first-order kinetics equation [39]. Figures 11 and 12 illustrate the linearized form of the pseudo-order model by using Equations (13) and (15) with changes in pH, highlighting the important effects of these parameters on photodegradation to remove organic pollutants from RWW. The adsorbent was investigated under specific conditions: 60 min reaction time. The results indicated that the

degradation rate increased with higher pH and $CoWO_4$/NCW at means the degradation rate increased with low pH, leading to the generation of more hydroxyl radicals, facilitating the oxidation of organic pollutants, and promoting the reaction. However, the increase in organic degradation was relatively modest, with the removal efficiency rising from 75.4% to 86% when the pH and $CoWO_4$/NCW dose were increased from 3 and 0.25 g to 9 and 1 g, respectively, as presented in Figures 13 and 14 [40].

Organic removal in wastewater involves complex reactions, making it challenging to differentiate individual reactions. Therefore, estimated kinetics for the degradation of organic solutions can be assumed, with many researchers reporting that most organic elimination curves adhere to first-order or second-order kinetics [41].

The kinetics study for $CoWO_4$/NCW with change the temperature, as illustrated in Figures 15 and 16 for first and second order respectively, revealed a fitting correlation between reaction time and the natural logarithm of the ratio C_t/C_o, indicative of a pseudo-first-order kinetic model. The organic removal kinetic report the degradation rate related to the uptake irradiation time. Once a target contaminant compound remains criticized through free radicals, three main mechanisms may remain complicated in the squalor of organics [42]. The rate constants for the first and second order for solar oxidation

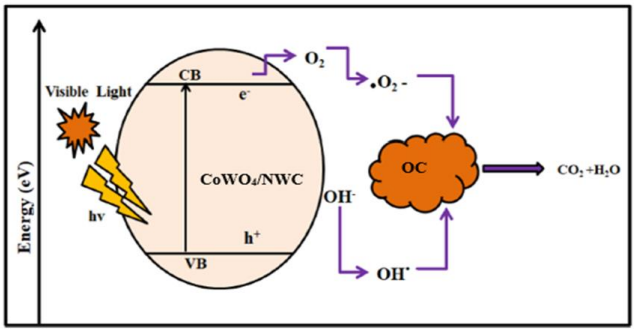

Figure 10. The potential mechanism of solar catalytic degradation

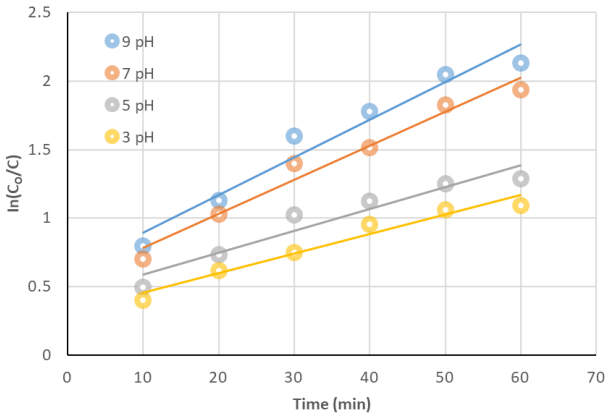

Figure 11. Plot of –ln (C/C_o) of $CoWO_4$/NCW vs. time

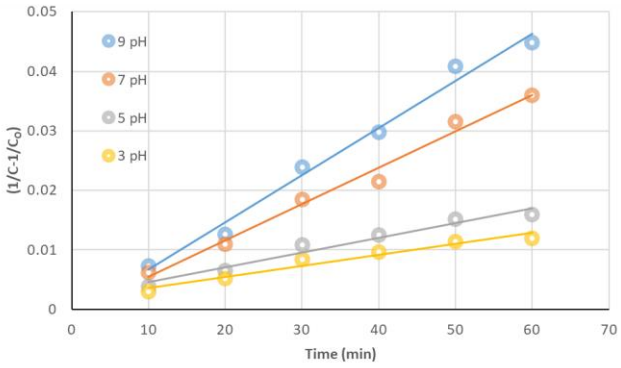

Figure 12. Pseudo second order model of $CoWO_4$/NCW vs. time

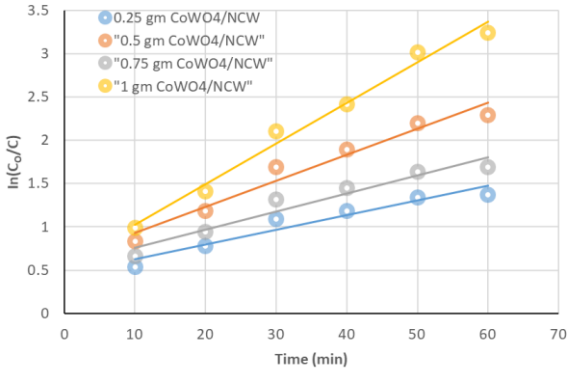

Figure 13. A plot of –ln (C/C_o) of $CoWO_4$/NCW vs. time

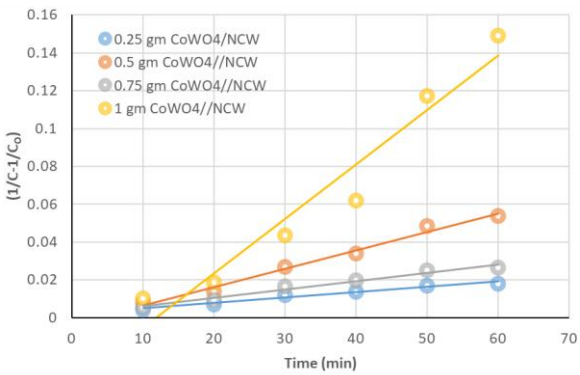

Figure 14. Pseudo second order model of $CoWO_4$/NCW vs. time

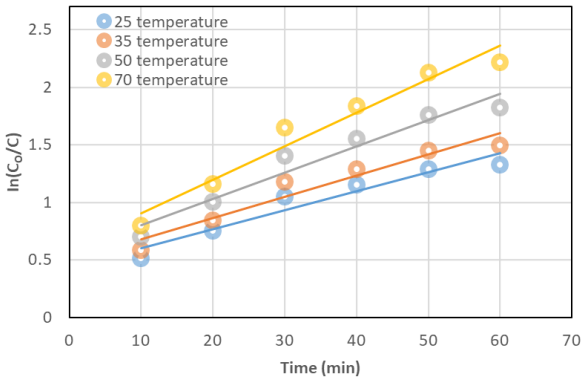

Figure 15. A plot of –ln (C/C_o) of $CoWO_4$/NCW vs. time

(CoWO4/NCW) were displayed in Tables 3, 4, and 5 for pH, dose, and temperature, respectively.

The pseudo-first-order equation can appropriate the data more than the pseudo-second-order equation, as shown by Tables 2 to 4, where R_2 for K_1 is greater than K_2, indicating that the rate of squalor was linear to the concentration of contaminant in refinery wastewater. These findings correspond to those made by [9]. and compared with similar works in Table 6. Table 6 presents a comparative analysis between the current work and other similar reported works, focusing on experimental parameters such as pollutant type, type and duration of irradiation, and the corresponding degradation percentages. It is noteworthy that the newly prepared composite photocatalyst exhibits promising performance compared to previously report conventional photocatalysts. This comparison highlights the effectiveness and potential of the synthesized composite photocatalyst in degrading pollutants under various experimental conditions, showcasing its superiority over existing conventional photocatalysts.The properties of clean water after treatment with CoWO4/NCW is 5.4 ppm organic pollutants, pH of 8, 5.21 NTU , 1.04 mPa/S, 223411 µs/cm, and 142983.04 ppm and compare with Table 1 for the refinery wastewater.

Table 3. Rate coefficients of pH experimentations

pH	CoWO4/NCW			
	First order		Second order	
	K_1	R^2	K_2	R^2
3	0.0139	0.9203	0.0002	0.9547
5	0.016	0.9264	0.0002	0.963
7	0.0248	0.9721	0.0006	0.9855
9	0.0275	0.9552	0.0008	0.9865

Table 4. Rate coefficients of dose experimentations

Dose (g)	CoWO4/NCW			
	First order		Second order	
	K_1	R^2	K_2	R^2
0.25	0.017	0.9308	0.0003	0.9674
0.5	0.021	0.9339	0.0004	0.9778
0.75	0.0301	0.9601	0.001	0.9866
1	0.0469	0.9853	0.0029	0.9434

4. Conclusion

In conclusion, the use of a novel composite material derived from cotton waste via acid hydrolysis with nitric acid, combined with cobalt tungstate, represents a promising approach for removing OP from RWW. The synergistic effects of CoWO4 and NCW lead to improved charge separation and photocatalytic activity under solar irradiation. The study demonstrates that the solar-assisted fabrication method for the CoWO4/NCW heterostructure is both efficient and scalable. The kinetics of the fabrication process show that solar energy can efficiently drive the synthesis reactions, resulting in a high-quality heterostructure with desirable properties.

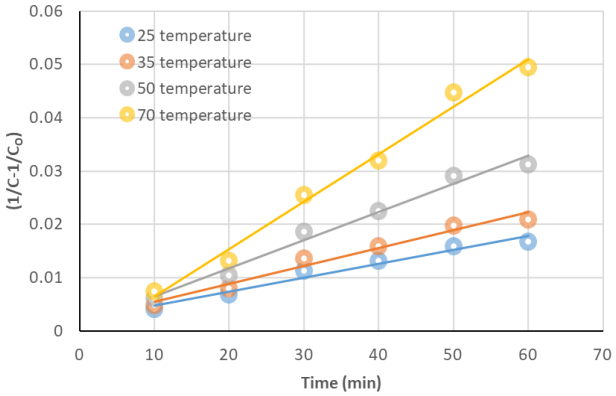

Figure 16. Pseudo second order model of CoWO4/NCW vs. time

Table 5. Rate coefficients of temperature experimentations

Temp (°C)	CoWO4/NCW			
	First order		Second order	
	K_1	R^2	K_2	R^2
25	0.0165	0.9276	0.0003	0.9645
35	0.0185	0.9332	0.0003	0.9711
50	0.0229	0.9445	0.0005	0.9815
70	0.0291	0.9568	0.0009	0.9872

Table 6. Comparison of the current study with other described studies

Photocatalyst	Organic Pollutants	Irradiation Type	Time (min)	Degradation Efficiency	Ref.
TiO2/Cellulose	Methyl Orange	Solar	30	92%	[17]
TiO2/ Cellulose Acetate	Antibacterial	UV	24	91.3%	[43]
ZnO/Cellulose	dyes	UV	20	75%	[44]
CoWO4/NCW	OP	Solar	120	97.4%	This work

Acknowledgements

We would like to express our sincere appreciation to the Department of Chemical Engineering, College of Engineering, University of Baghdad, for their unwavering support and generous provision of resources, without which this research would not have been feasible. Their invaluable expertise and guidance have been instrumental in our accomplishments, underscoring their pivotal role in the success of this endeavor.

CRediT Author Statement

Ali Hassan. conceptualized and designed the work, shared the investigation data examination, and manuscript preparation and editing. Ibtehal Kareem achieved the experiments and contributed to data analysis and manuscript writing. All authors have read and decided on the published version of the manuscript.

References

[1] Ahmed, M.J., Mohammed, A.H.A.K., Kadhum, A.A.H. (2011). Modeling of Breakthrough Curves for Adsorption of Propane, n-Butane, and Iso-Butane Mixture on 5A Molecular Sieve Zeolite. *Transp. Porous Media*, 86, 1, 215–228. DOI: 10.1007/s11242-010-9617-5

[2] Hassan, A.A., Al-Zobai, K.M.M. (2019). Chemical oxidation for oil separation from oilfield-produced water under UV irradiation using titanium dioxide as a nano-photocatalyst by batch and continuous techniques. *Int. J. Chem. Eng.*, 2019. DOI: 10.1155/2019/9810728

[3] Ibrahim, H.A., Hassan, A.A., Ali, A.H., Kareem, H.M. (2023). Organic removal from refinery wastewater by using electrocatalytic oxidation. *AIP Conference Proceedings*, AIP Publishing. DOI: 10.1063/5.0163257

[4] Anastopoulos, I., Ahmed, M.J., Ojukwu, V.E., Danish, M.M., Ighalo, J.O. (2023). A comprehensive review on adsorption of Reactive Red 120 dye using various adsorbents. *J. Mol. Liq.*, 123719, DOI: 10.1016/j.molliq.2023.123719

[5] Ahmed, M.J., Anastopoulos, I., Kalderis, D., Haris, M., Usman, M. (2024). Insight into the wheat residues-derived adsorbents for the remediation of organic and inorganic aquatic contaminants: A review. *Environ. Res.*, 118507. DOI: 10.1016/j.envres.2024.118507

[6] Attaeyan, A., Shahgholi, M., Khandan, A. (2023). Fabrication and Characterization of Novel 3D Porous Titanium-6Al-4V Scaffold for Orthopedic Application Using Selective Laser Melting Technique. *Iran. J. Chem. Chem. Eng*, 43, 1, 21–37. DOI: 10.30492/IJCCE.2023.1991010.5905

[7] Jasim, M., AlJaberi F.Y. (2022) Investigation of oil content removal performance in real oily wastewater treatment by electrocoagulation technology: RSM design approach. *Results Eng.*, 18, 101082. DOI: 10.1016/j.rineng.2023.101082.

[8] AlJaberi, F.Y., Abdulmajeed, B.A., Hassan, A.A., Ghadban, M.L. (2020). Assessment of an Electrocoagulation Reactor for the Removal of Oil Content and Turbidity from Real Oily Wastewater Using Response Surface Method. *Recent Innov. Chem. Eng.* (Formerly Recent Patents Chem. Eng., 13, 1, 55–71, DOI: 10.2174/2405520412666190830091842

[9] Nawaf, A.T., Hameed, S.A., Abdulateef, L.T., Jarullah, A.T., Kadhim, M.S. Mujtaba, I. M. (2021) A novel synthetic nano-catalyst (Ag2O3/Zeolite) for the high quality of light naphtha by batch oxidative desulfurization reactor. *Bull. Chem. React. Eng. Catal.*, 16 (4), 716–732, DOI: 10.9767/bcrec.16.4.11383.716-732

[10] Raheem, S., Al-yaqoobi, A., Znad, H., Abid, H.R. (2024). Caffeine Extraction from Spent Coffee Grounds by Solid-liquid and Ultrasound-assisted Extraction: Kinetic and Thermodynamic Study. *Iraqi J. Chem. Pet. Eng.*, 25, 1, 49–57. DOI: 10.31699/ijcpe.2024.1.5

[11] Nawaf, A.T., Jarullah, A.T., Abdulateef, L.T. (2019). Design of a synthetic zinc oxide catalyst over nano-alumina for sulfur removal by air in a batch reactor. *Bull. Chem. React. Eng. Catal.*, 14 (1), 79-92. DOI: 10.9767/bcrec.14.1.2507.79-92

[12] Alamery, H.R.D., Hassan, A.A., Rashid, A.H. (2023). Copper Removal in Simulated Wastewater by Solar Fenton Oxidation *AIP Conf. Proc.*, 2806 (1), DOI: 10.1063/5.0167259

[13] Al-Jubouri, S.M., Sabbar, H.A., Lafta, H.A., Waisi, B.I. (2019). Effect of synthesis parameters on the formation 4a zeolite crystals: Characterization analysis and heavy metals uptake performance study for water treatment. *Desalin. Water Treat.*, 165, 290–300. DOI: 10.5004/dwt.2019.24566

[14] Bano, K.S., Mittal, K., Singh, P.P., Kaushal, S. (2021). Nanoscale Advances Sunlight driven photocatalytic degradation of degradation pathways. *Nanoscale Adv.*, 3, 6446–6458. DOI: 10.1039/D1NA00499A

[15] Ashiegbu, D.C., Potgieter, H.J. (2023) ZnO-based heterojunction catalysts for the photocatalytic degradation of methyl orange dye. *Heliyon*, 9 (10), e20674. DOI: 10.1016/j.heliyon.2023.e20674

[16] Al-Jubouri, S.M., Sabbar, H.A., Khudhair, E.M., Ammar, S.H., Al Batty, S., Khudhair, S.Y., Mahdi, A.S. (2023) Chemistry Silver oxide-zeolite for removal of an emerging contaminant by simultaneous adsorption-photocatalytic degradation under simulated sunlight irradiation. *J. Photochem. Photobiol. A Chem.*, 442, 114763. DOI: 10.1016/j.jphotochem.2023.114763.

[17] Jothivenkatachalam, K., Prabhu, S., Nithya, A., Chandra Mohan, S., Jeganathan, K. (2015). Solar, visible, and UV light photocatalytic activity of CoWO4 for the decolorization of methyl orange. *Desalin. Water Treat.*, 54 (11), 3134–3145. DOI: 10.1080/19443994.2014.906324

[18] Ayad, M.M., Elmorsy, E., Amer, W.A., Mahrous, A. (2022) Insight into the Novel Zif-8@N-Cqds/Zif-67 Nanocomposite for Photocatalytic Degradation of Methylene Blue Under Visible Light Irradiation. *SSRN Electron. J.*, 1–24. DOI: 10.2139/ssrn.4286781

[19] Atiyah, A.S., Al-Samawi, A.A.A., Hassan, A.A. (2020) Photovoltaic cell electro-Fenton oxidation for treatment of oily wastewater. *AIP Conf. Proc.*, 2235. DOI: 10.1063/5.0008937

[20] Theivasanthi, T., Christma, F.L., Joshua, A.A., Gopinath, S.C.B. (2018) Synthesis and characterization of cotton fiber-based nanocellulose. *International Journal of Biological Macromolecules*, 109, 832–836 . DOI: 10.1016/j.ijbiomac.2017.11.054

[21] Zang, N., Qian, X. (2012). Influence of organic acid on the thermal hazard of hydrogen peroxide. *Procedia Eng.*, 45, 526–532. DOI: 10.1016/j.proeng.2012.08.198

[22] Flihh, S.M., Ammar, S.H. (2021) Fabrication and photocatalytic degradation activity of core/shell ZIF-67@CoWO4@CoS heterostructure photocatalysts under visible light. *Environ. Nanotechnology, Monit. Manag.*, 16, 100595. DOI: 10.1016/j.enmm.2021.100595

[23] Abdul Majeed, B.A., Sabar, D.A. (2017) Preparations of Organoclay Using Cationic Surfactant and Characterization of PVC/ (Bentonite and Organoclay) Composite Prepared via Melt Blending Method. *Iraqi J. Chem. Pet. Eng.*, 18 (1), 17–36. DOI: 10.31699/ijcpe.2017.1.2

[24] Nawaf, A.T., Abdulmajeed, B.A. (2024). Design of oscillatory helical baffled reactor and dual functional mesoporous catalyst for oxidative desulfurization of real diesel fuel. *Chem. Eng. Res. Des.*, 209, 193–209. DOI: 10.1016/j.cherd.2024.07.032

[25] Mhawesh, T.H., Abd Ali, Z.T. (2020) Reuse of Brick Waste as a cheap sorbent for the Removal of Nickel Ions from Aqueous Solutions. *Iraqi J. Chem. Pet. Eng.*, 21 (2), 15–23. DOI: 10.31699/ijcpe.2020.2.3

[26] Shekofteh-Gohari M., Habibi-Yangjeh, A. (2017). Fe3O4/ZnO/CoWO4 nanocomposites: Novel magnetically separable visible-light-driven photocatalysts with enhanced activity in the degradation of different dye pollutants. *Ceram. Int.*, 43 (3), 3063–3071 DOI: 10.1016/j.ceramint.2016.11.115

[27] Alfattal, A.H., Abbas, A.S. (2019) Synthesized 2nd Generation Zeolite as an Acid-Catalyst for Esterification Reaction. *Iraqi J. Chem. Pet. Eng.*, 20 (3), 67–73. DOI: 10.31699/ijcpe.2019.3.9

[28] Simayee, M., Iraji zad, A., Esfandiar, A. (2023) Green synthesis of copper nanoparticles on the cotton fabric as a self-regenerating and highly efficient plasmonic solar evaporator. *Sci. Rep.*, 13 (1), 1–11. DOI: 10.1038/s41598-023-40060-5

[29] Nidheesh, P.V., Gandhimathi, R. (2015) Textile Wastewater Treatment by Electro-Fenton Process in Batch and Continuous Modes. *J. Hazardous, Toxic, Radioact. Waste*, 19 (3), 04014038. DOI: 10.1061/(asce)hz.2153-5515.0000254

[30] Nawaf, A.T., Abdulmajeed, B.A. (2024). Synthesis of a Fe2O3-supported composite for rapid oxidative desulfurization production of environmentally friendly fuel in an OBR. *Int. J. Environ. Sci. Technol.*, 0123456789. DOI: 10.1007/s13762-024-05920-1

[31] Bali, U., Çatalkaya, E., Şengül, F. (2004). Photodegradation of reactive black 5, direct red 28 and direct yellow 12 using UV, UV/H22 and UV/H2O2/Fe2+: A comparative study. *J. Hazard. Mater.*, 114 (1–3), 159–166. DOI: 10.1016/j.jhazmat.2004.08.013

[32] Naser, G.F., Dakhil, I.H., Hasan, A.A. (2024) Evaluation of Electro-Fenton Process for Removal of Amoxicillin from Evaluation of electro-fenton process for removal of amoxicillin from simulated wastewater. *Glob. NEST J.* DOI: 10.30955/gnj.006075

[33] Nsaif, R.D., Alturki, S.F., Suwaed, M.S., Hassan, A.A. (2023). Lead removal from refinery wastewater by using photovoltaic electro Fenton oxidation. *AIP Conference Proceedings*. DOI: 10.1063/5.0163378

[34] Amor, C., Marchão, L., Lucas, M. S. Peres, J.A. (2019) Application of advanced oxidation processes for the treatment of recalcitrant agro-industrial wastewater: A review. *Water (Switzerland)*, 11 (2). DOI: 10.3390/w11020205

[35] Levien, K.L., Levenspiel, O. (1999). Optimal product distribution from laminar flow reactors: Newtonian and other power-law fluids. *Chem. Eng. Sci.*, 54, (13–14), 2453–2458. DOI: 10.1016/S0009-2509(98)00484-9.

[36] Sun, J.H., Sun, S.P., Fan, M.H., Guo, H.Q., Qiao, L.P., Sun, R.X. (2007). A kinetic study on the degradation of p-nitroaniline by Fenton oxidation process. *J. Hazard. Mater.*, 148 (1–2), 172–177. DOI: 10.1016/j.jhazmat.2007.02.022

[37] Khalaf, R.M., Kariem, N.O., Khudhair, A.A.M. (2018) Removal of Textile Dye from Aqueous Media Using an Advanced Oxidation Process with UV/H2O2,. *IOP Conf. Ser. Mater. Sci. Eng.*, 433 (1). DOI: 10.1088/1757-899X/433/1/012039

[38] Somwanshi, S.B., Kharat, P.B. (2020) Nanocatalyst: A brief review on synthesis to applications. *J. Phys. Conf. Ser.*, 1644 (1). DOI: 10.1088/1742-6596/1644/1/012046

[39] Pal, D.B., Lavania, R., Srivastava, P., Singh, P., Srivastava, K.R., Madhav, S., Mishra, P.K. (2018). Photocatalytic degradation of methyl tertiary butyl ether from wastewater using CuO/CeO2 composite nanofiber catalyst. *J. Environ. Chem. Eng.*, 6 (2), 2577–2587. DOI: 10.1016/j.jece.2018.04.001

[40] Teymori, M., Khorsandi, H., Aghapour, A.A., Jafari, S.J., Maleki, R. (2020) Electro-Fenton method for the removal of Malachite Green: effect of operational parameters. *Appl. Water Sci.*, 10 (1). DOI: 10.1007/s13201-019-1123-5

[41] Al-Jaberi, F.Y. (2023). Treatment of Refinery Wastewater by Chemical Advanced Oxidation Processes (UV-photolysis, Fenton, and photo-Fenton): A Comparative Study. *Iran. J. Chem. Chem. Eng.*, 42 (8), 2708–2718. DOI: 10.30492/ijcce.2023.560200.5520

[42] Agarwal, S., Tyagi, I., Gupta, V.K., Ghasemi, N., Shahivand, M., Ghasemi, M. (2016). Kinetics, equilibrium studies, and thermodynamics of methylene blue adsorption on Ephedra strobilacea sawdust and modified using phosphoric acid and zinc chloride. *J. Mol. Liq*., 218, 208–218. DOI: 10.1016/j.molliq.2016.02.073

[43] Kamel., S. (2022) Recent Development of Cellulose/TiO2 Composite in Water Treatment. *Egypt. J. Chem*., 65 (13), 601–612. DOI: 10.21608/ejchem.2022.128431.5689

[44] Abu-dalo, M.A., Al-rosan, S.A., Albiss, B.A. (2021). Photocatalytic Degradation of Methylene Blue Using Polymeric Membranes Based on Cellulose Acetate Impregnated with ZnO Nanostructures.Polymers (Basel), 1–17. DOI: 10.3390/polym13193451